Supporting information: TD-DFT Study of the Light-induced Spin Crossover of Fe(III) Complexes

Sergi Saureu,[a] Coen de Graaf[a,b]

[a]Departament de Química Física i Inorgànica,
Universitat Rovira i Virgili, Marcel·lí Domingo s/n,
43007 Tarragona, Spain. E-mail: coen.degraaf@urv.cat

[b]Institució Catalana de Recerca i Estudis Avançats (ICREA)
Passeig Lluis Companys 23, 08010 Barcelona, Spain

April 1, 2016

Contents

S1 $[Fe(qsal)_2]^+$: complete active space orbitals, CAS(13,14). 3

S2 $[Fe(qsal)_2]^+$: Selected B3LYP* angles. 5

S3 $[Fe(qsal)_2]^+$: Selected PBE0 distances, angles, energies and vibrations. 7

S4 $[Fe(pap)_2]^+$: complete active space orbitals, CAS(13,14). 10

S5 $[Fe(pap)_2]^+$: Selected B3LYP* angles. 12

S1 $[Fe(qsal)_2]^+$: complete active space orbitals, CAS(13,14).

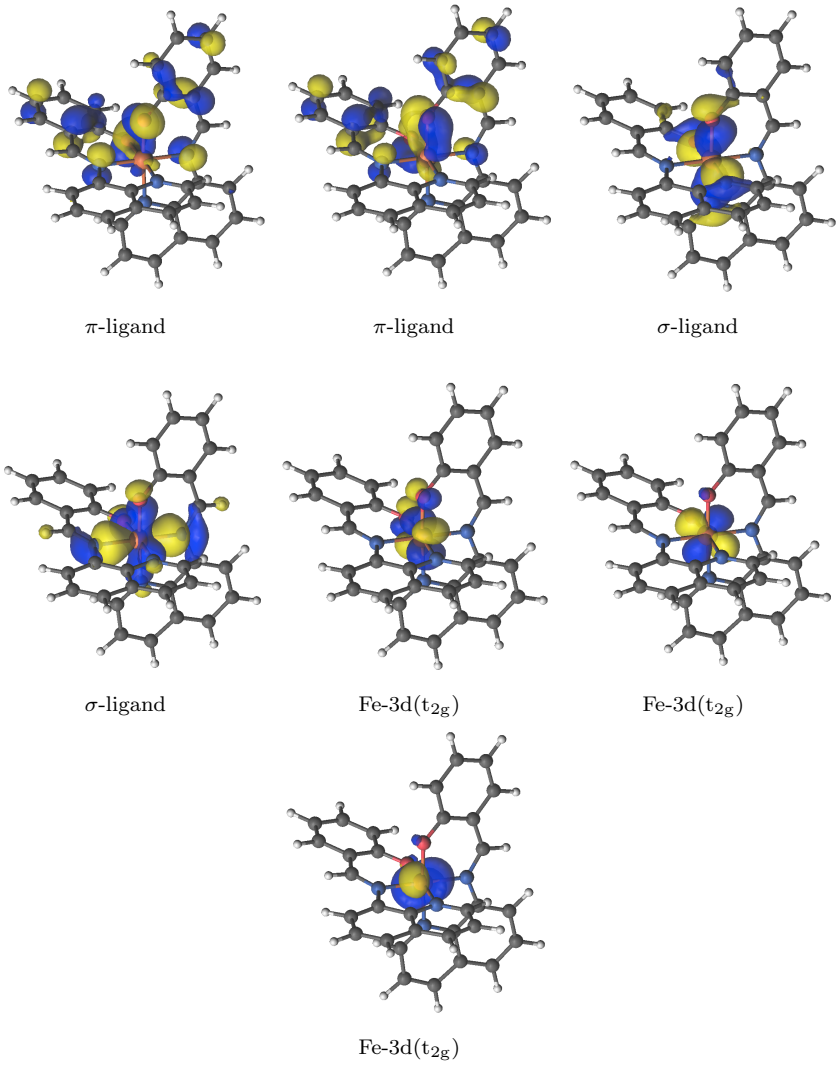

Figure S1.1: CAS(13,14) orbitals. For CAS(9,12) the π orbitals are not included in the active space.

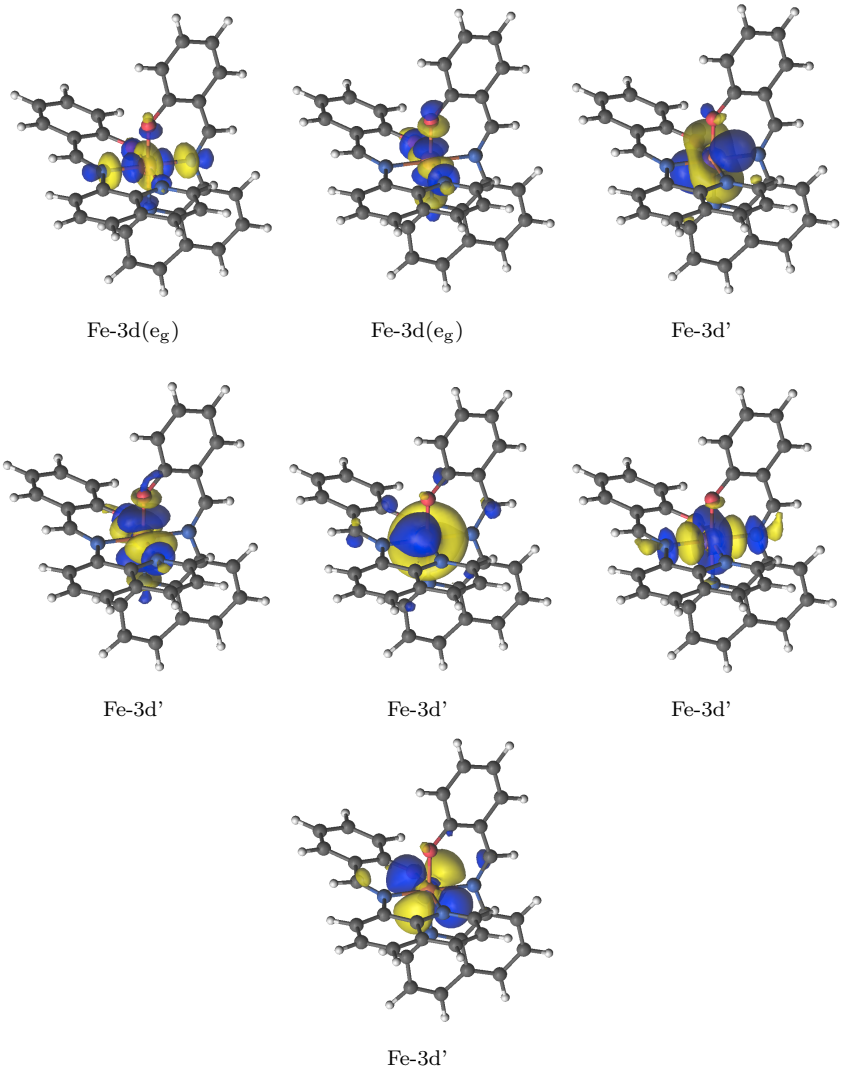

Figure S1.1: (*Continued*) CAS(13,14) orbitals. For CAS(9,12) the π orbitals are not included in the active space.

S2 $[Fe(qsal)_2]^+$: Selected B3LYP* angles.

Table S2.1: B3LYP*/def2-TZVP optimized angles. The experimental distances in parenthesis are taken from [Hayami *et al.*, *J. Am. Chem. Soc.* **2001**, 123, 11644–11650].

angle	LS	HS	$\Delta \measuredangle$
O(1)–Fe(1)–O(2)	93.4 (93.8)	96.7 (98.2)	3.3 (4.4)
O(1)–Fe(1)–N(1)	93.7 (94.7)	86.3 (97.1)	7.4 (2.4)
O(1)–Fe(1)–N(2)	175.0 (175.7)	161.3 (165.2)	13.7 (10.5)
O(1)–Fe(1)–N(3)	87.1 (85.3)	103.6 (89.1)	16.5 (3.8)
O(1)–Fe(1)–N(4)	89.2 (90.4)	90.0 (89.8)	0.8 (0.6)
O(2)–Fe(1)–N(1)	87.1 (86.6)	103.6 (89.1)	16.5 (2.5)
O(2)–Fe(1)–N(2)	89.2 (89.9)	89.9 (89.8)	0.7 (0.1)
O(2)–Fe(1)–N(3)	93.7 (94.5)	86.3 (97.1)	7.4 (2.6)
O(2)–Fe(1)–N(4)	175.0 (175.1)	161.3 (165.2)	13.7 (9.9)
N(1)–Fe(1)–N(2)	82.2 (83.3)	75.2 (95.5)	7.0 (12.2)
N(1)–Fe(1)–N(3)	178.9 (179.0)	165.3 (170.5)	13.6 (8.5)
N(1)–Fe(1)–N(4)	96.9 (95.6)	94.2 (77.4)	2.7 (18.2)
N(2)–Fe(1)–N(3)	96.9 (96.6)	94.1 (77.4)	2.8 (19.2)
N(2)–Fe(1)–N(4)	88.5 (86.0)	89.1 (85.4)	0.6 (0.6)
N(3)–Fe(1)–N(4)	82.2 (83.3)	75.2 (95.5)	7.0 (12.2)

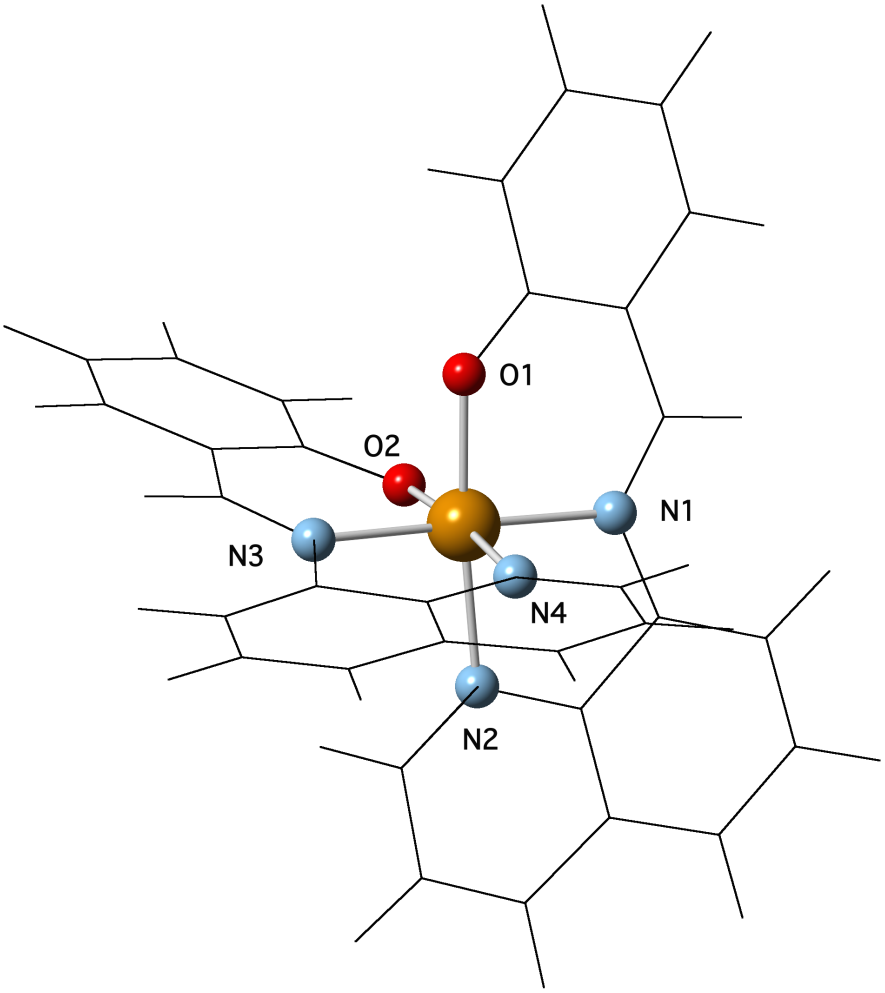

Figure S2.1: Atom numbering of the $[Fe(qsal)_2]^+$used in Table S2.1.

S3 $[Fe(qsal)_2]^+$: Selected PBE0 distances, angles, energies and vibrations.

Table S3.1: PBE0/def2-TZVP optimized bond lengths in Å of complex $[Fe(qsal)_2]^+$. The B3LYP* distances are taken from this work and experimental distances from [Hayami *et al.*, *J. Am. Chem. Soc.* **2001**, 123, 11644–11650].

distance	HS	LS	Δr
		PBE0	
Fe–O	1.91	1.86	0.05
Fe–N_1	2.19	2.00	0.19
Fe–N_2	2.13	1.95	0.18
		B3LYP*	
Fe–O	1.91	1.88	0.03
Fe–N_1	2.21	2.02	0.19
Fe–N_2	2.18	1.97	0.21
		Experimental	
Fe–O	1.88	1.88	0.00
Fe–N_1	2.12	1.97	0.15
Fe–N_2	2.09	1.94	0.25

Table S3.2: PBE0/def2-TZVP optimized angles. B3LYP* values in parenthesis are given for comparison.

angle	LS	HS	$\Delta \measuredangle$
O(1)–Fe(1)–O(2)	94.4 (93.4)	97.3 (96.7)	2.9 (3.3)
O(1)–Fe(1)–N(1)	93.6 (93.7)	86.3 (103.5)	7.3 (7.4)
O(1)–Fe(1)–N(2)	174.3 (175.0)	161.2 (161.3)	13.1 (13.7)
O(1)–Fe(1)–N(3)	86.6 (87.1)	101.1 (86.3)	14.5 (16.5)
O(1)–Fe(1)–N(4)	89.3 (89.2)	90.4 (90.0)	1.1 (0.8)
O(2)–Fe(1)–N(1)	86.6 (87.1)	100.6 (86.3)	14 (16.5)
O(2)–Fe(1)–N(2)	89.3 (89.2)	90.9 (89.9)	1.6 (0.7)
O(2)–Fe(1)–N(3)	93.6 (93.7)	86.4 (103.6)	7.2 (7.4)
O(2)–Fe(1)–N(4)	174.3 (175.0)	161.4 (161.3)	12.9 (13.7)
N(1)–Fe(1)–N(2)	82.3 (82.2)	75.5 (94.2)	6.8 (7)
N(1)–Fe(1)–N(3)	178.9 (178.9)	169.1 (165.3)	9.8 (13.6)
N(1)–Fe(1)–N(4)	97.5 (96.9)	96.7 (75.2)	0.8 (2.7)
N(2)–Fe(1)–N(3)	97.5 (96.9)	96.7 (75.2)	0.8 (2.8)
N(2)–Fe(1)–N(4)	87.4 (88.5)	87.0 (89.1)	0.4 (0.6)
N(3)–Fe(1)–N(4)	82.3 (82.2)	75.5 (94.1)	6.8 (7)

Table S3.3: Adiabatic HS-LS energy difference (ΔE_{HL}) and difference in zero-point energy (ΔZPE) at PBE0/def2-TZVP level. Energies in cm^{-1}. B3LYP* values are given for comparison.

	$[Fe(qsal)_2]^+$	
	PBE0	B3LYP*
ΔE_{HL}	-1380	2166
ΔZPE	-590	-670
ΔH_{HL}	-1970	1496

Table S3.4: Frequencies in cm^{-1} of the Fe-L bending and stretching modes for the LS and HS states of $[Fe(qsal)_2]^+$at PBE0 level. The labels of the stretching modes are approximate due to the non-ideal octahedral symmetry. B3LYP* values are given for comparison.

	$[Fe(qsal)_2]^+$			
	PBE0		B3LYP*	
Character	LS	HS	LS	HS
Bending				
	166	138	164	133
	186	147	184	141
	201	186	200	185
	224	195	224	193
	235	212	233	210
Stretching				
e_g	223	218	218	222
e_g	261	225	256	239
a_g	263	230	259	226
t_{1u}	350	265	342	260
t_{1u}	361	275	353	261
t_{1u}	397	317	385	308

S4 $[Fe(pap)_2]^+$: complete active space orbitals, CAS(13,14).

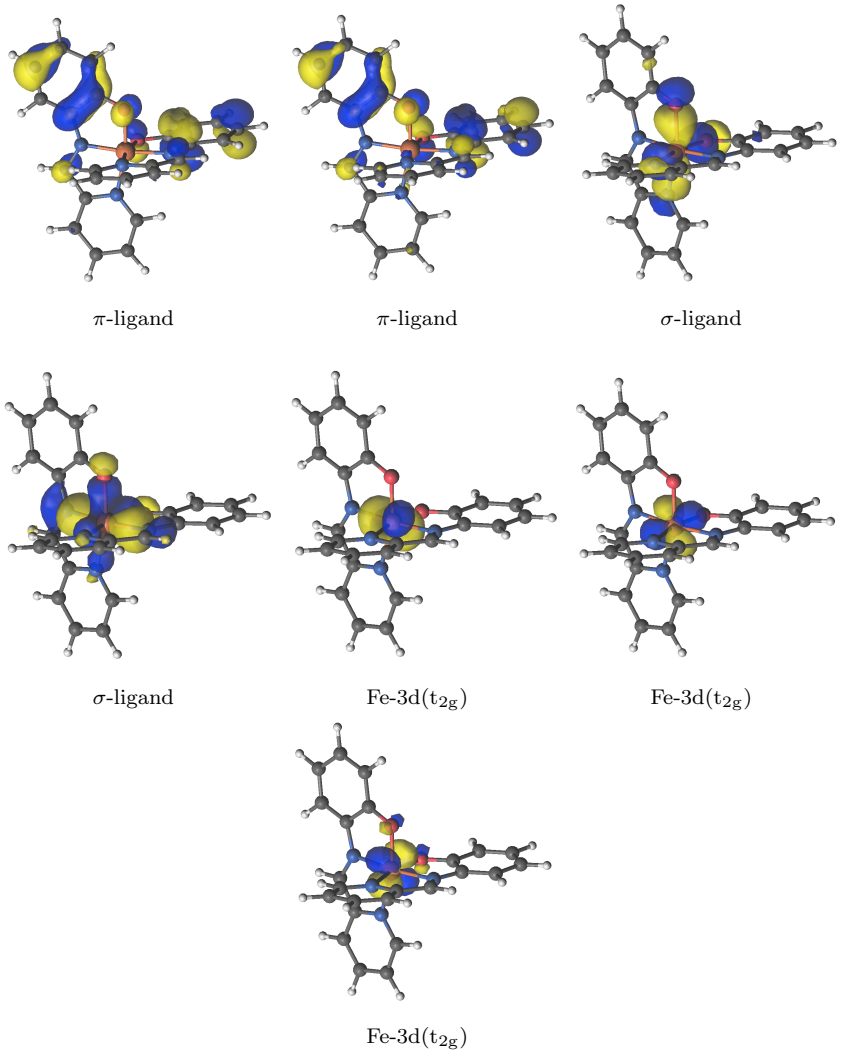

Figure S4.1: CAS(13,14) orbitals. For CAS(9,12) the π orbitals are not included in the active space.

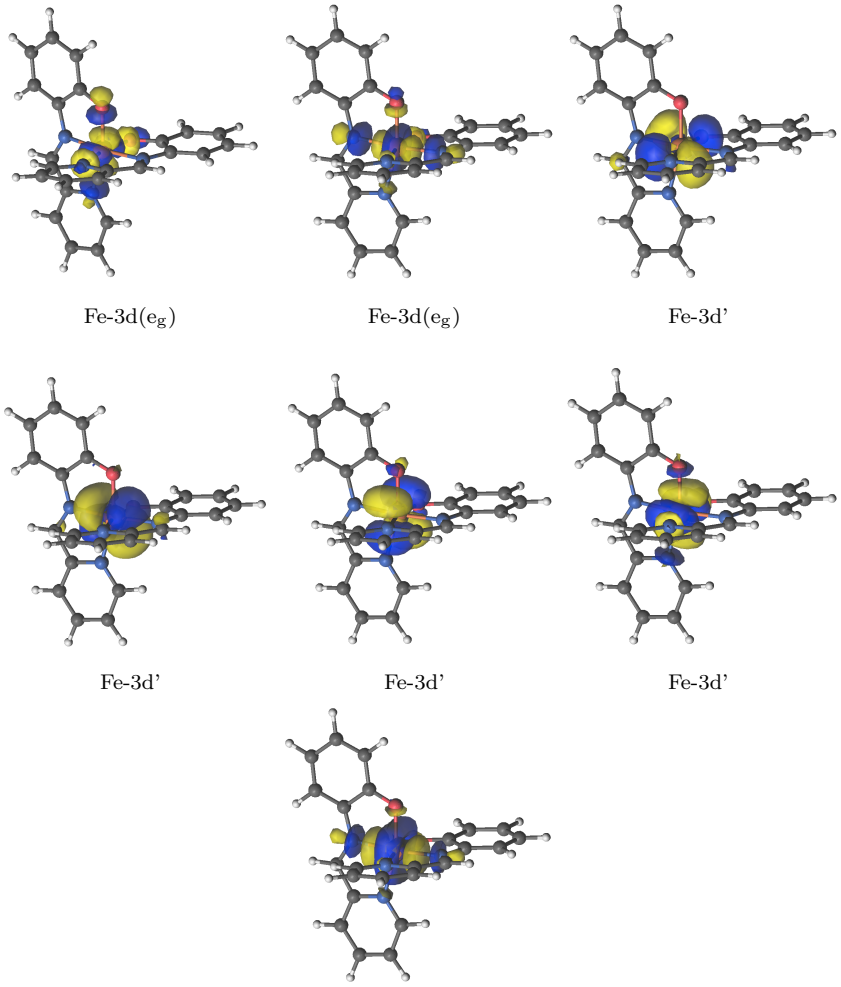

Figure S4.1: (*Continued*) CAS(13,14) orbitals. For CAS(9,12) the π orbitals are not included in the active space.

S5 $[Fe(pap)_2]^+$: Selected B3LYP* angles.

Table S5.1: B3LYP*/def2-TZVP optimized angles. The experimental distances in parenthesis are taken from [Hayami *et al.*, *Chem. Eur. J.* **2009**, 15, 3497–3508].

angle	LS	HS	$\Delta \measuredangle$
O(1)–Fe(1)–O(2)	94.8 (93.6)	101.1 (96.0)	6.3 (2.4)
O(1)–Fe(1)–N(1)	84.9 (85.7)	77.6 (79.0)	7.3 (6.7)
O(1)–Fe(1)–N(2)	166.1 (166.4)	150.3 (152.8)	15.8 (13.6)
O(1)–Fe(1)–N(3)	90.8 (92.0)	114.2 (110.9)	23.4 (18.9)
O(1)–Fe(1)–N(4)	89.8 (90.5)	91.0 (94.3)	1.2 (3.8)
O(2)–Fe(1)–N(1)	90.3 (91.6)	102.2 (115.1)	11.9 (23.5)
O(2)–Fe(1)–N(2)	87.9 (90.0)	89.9 (92.0)	2.0 (2.0)
O(2)–Fe(1)–N(3)	85.0 (85.7)	77.4 (79.2)	7.6 (6.5)
O(2)–Fe(1)–N(4)	165.7 (166.4)	150.7 (152.7)	15.0 (13.7)
N(1)–Fe(1)–N(2)	81.4 (81.0)	73.1 (74.1)	8.3 (6.9)
N(1)–Fe(1)–N(3)	173.4 (176.4)	168.2 (162.3)	5.2 (14.1)
N(1)–Fe(1)–N(4)	103.7 (101.7)	95.0 (91.7)	8.7 (10.0)
N(2)–Fe(1)–N(3)	103.0 (101.4)	106.5 (96.1)	3.5 (5.3)
N(2)–Fe(1)–N(4)	90.9 (89.0)	92.5 (90.4)	1.6 (1.4)
N(3)–Fe(1)–N(4)	81.3 (81.1)	73.2 (73.5)	8.1 (7.6)

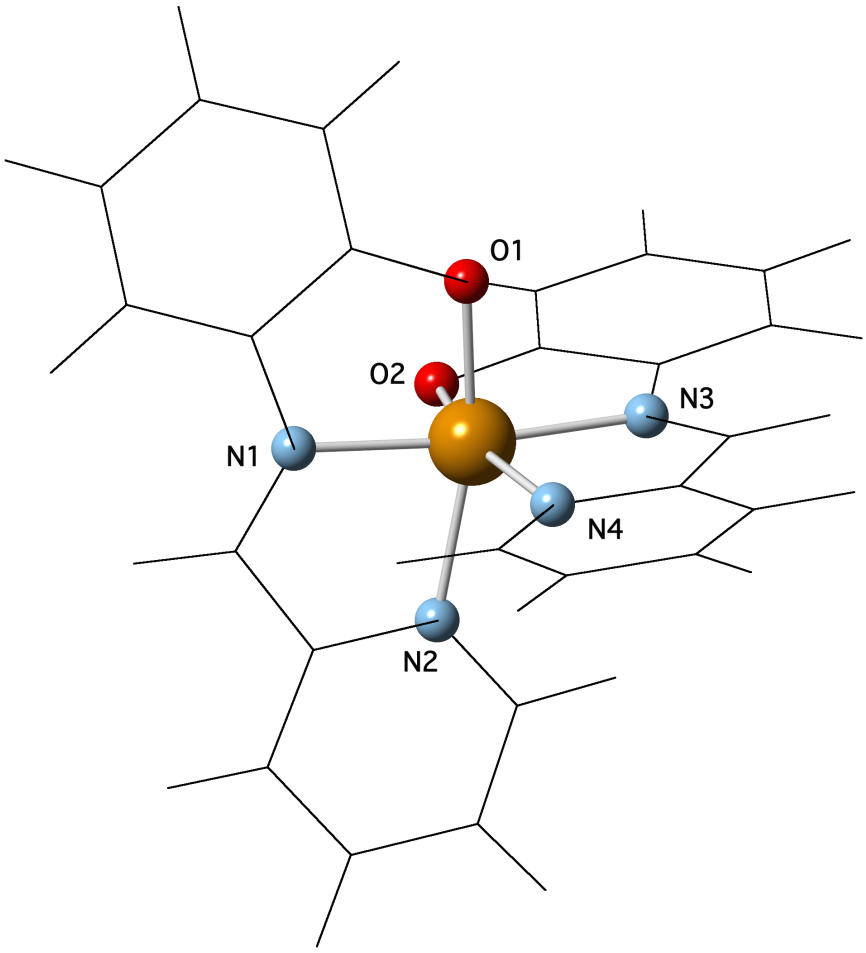

Figure S5.1: Atom numbering of the $[Fe(pap)_2]^+$used in Table S5.1.